

Spin-wave hybridization and magnetic anisotropies in a thick bcc cobalt film

X. Liu, R. L. Stamps, and R. Sooryakumar

Department of Physics, The Ohio State University, Columbus, Ohio 43210

G. A. Prinz

Naval Research Laboratory, Washington, D.C. 20375

(Received 13 March 1996; revised manuscript received 8 August 1996)

Magnetic anisotropies of a 357 Å thick Co film were examined using Brillouin light scattering. The Co has bcc structure, and was found to have a significant fourfold anisotropy in addition to a strong uniaxial anisotropy. This film is one of the thickest bcc Co structures and we find that the surface and $n=1$ bulk spin waves have comparable frequencies and are strongly mixed. Unusual behavior of the scattering intensities suggest the possible presence of inhomogeneous internal fields that result in a different dependence for the bulk mode frequencies on field orientation than for the surface mode. [S0163-1829(96)09242-9]

The Co bcc structure has received a great deal of attention, with some controversy regarding the stability of the bcc state.¹⁻³ Predictions exist for a metastable bcc phase, with a large exchange splitting between majority and minority spin bands, and also as a state forced by substrate matching.⁴⁻⁶ In this paper we report magnetization, exchange, and anisotropy parameters for one of the thickest existing bcc Co films, as determined using Brillouin light scattering methods.⁷⁻⁹

Previous examinations of bcc Co films revealed uniaxial anisotropies for 202 and 216 Å thicknesses.⁸ These films were grown on (100) and (110) substrates and displayed significantly different magnitudes for anisotropies. The results were consistent with a possible magnetoelastic origin for the anisotropy arising from lattice mismatch at the interface with the substrate. Although a fourfold anisotropy consistent with a cubic symmetry was observed in one film, its magnitude was small.

Our present results indicate a much larger negative fourfold anisotropy in addition to a large uniaxial anisotropy. Furthermore, curious Stokes/anti-Stokes ratios for strongly hybridized surface and $n=1$ bulk modes suggest possible surface "pinning" effects that could be caused by inhomogeneities in the internal effective fields near the surfaces.¹⁰

The sample was a single crystal 357 Å film of (110) bcc Co grown on GaAs by molecular-beam epitaxy.¹ The film thickness was determined by x-ray fluorescence to within $\pm 5\%$. Results obtained with x-ray diffraction¹ and surface-enhanced x-ray-absorption fine-structure¹¹ (EXAFS) studies were consistent with a bcc structure. Brillouin spectra were taken at room temperature using 100 mW of p -polarized 5145 Å laser at 30° angle of incidence. The s -polarized backscattered light was analyzed with a six-pass tandem Fabry-Pérot interferometer.

Spin-wave frequencies and scattering intensities were measured in three different series of experiments: as a function of orientation angle ϕ_H between the applied field and the [100] direction and as a function of field along hard and easy directions (the geometry is shown in Fig. 1). The magnetization was measured using a superconducting quantum interference device (SQUID) magnetometer and $4\pi M_S$ was found to be 14.3 ± 0.7 kG at room temperature.

The calculations involve the following steps:¹²⁻¹⁴ (1) finding the equilibrium orientation of the magnetization determined by competition between anisotropies and the applied magnetic field; (2) forming equations of motion from torques acting on the spins deviated slightly from equilibrium; and (3) solving the linearized equations of motion, together with appropriate electromagnetic and exchange boundary conditions, for the frequencies of long wavelength spin waves in a film geometry.

The presence of anisotropy fields within the film cause the magnetization in general to be noncollinear with H_0 when the field is not applied along a symmetry direction.¹⁵ The equilibrium orientation of the magnetization is found by minimizing the total energy with respect to ϕ . Assuming the film is magnetized in-plane, the energy E for the static orientation is given by

$$E = -H_0 M_S \cos(\phi_H - \phi) + (K_1/4) \times [1 - \sin^2 \phi + (3/4) \sin^2 2\phi] - K_u \cos^2 \phi. \quad (1)$$

This energy is appropriate for (110) surfaces where K_1 is the fourfold crystalline anisotropy and K_u is a uniaxial in-plane anisotropy. An additional uniaxial out-of-plane anisotropy

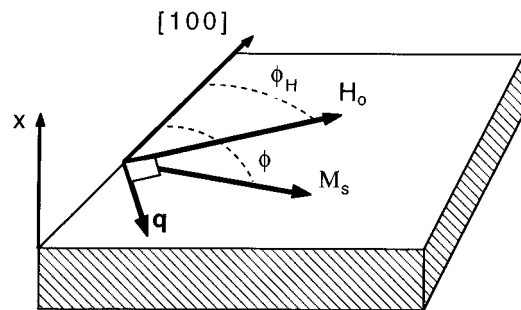


FIG. 1. Scattering geometry. The angle ϕ_H measures the orientation of the in-plane applied field H_0 relative to the [100] direction. The angle between the magnetization and the [100] direction is given by ϕ . The in-plane propagation wave vector q is always perpendicular to the field.

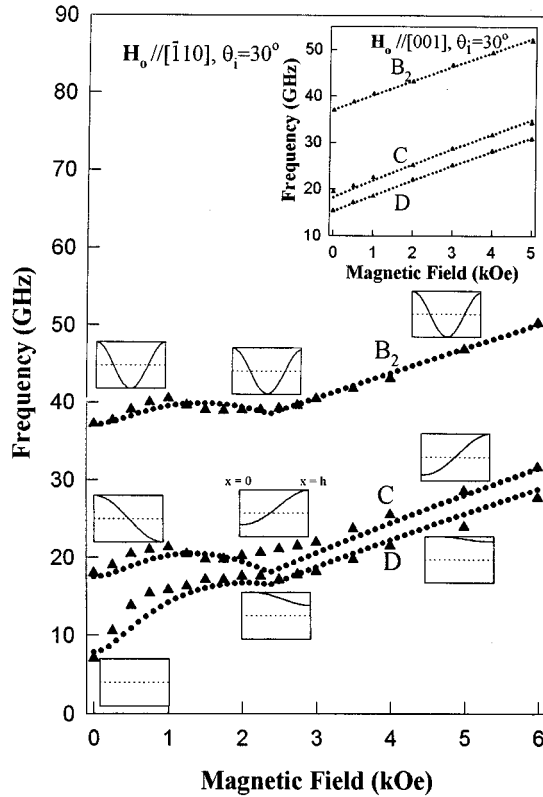


FIG. 2. Magnetic field (H_0) dependence of the three lowest spin-wave frequencies. The main figure shows the frequencies of modes when H_0 is along the hard axis $[\bar{1}10]$ and the inset shows when H_0 is parallel to the easy axis $[001]$. The angle of incidence θ_i was 30° . The dotted lines are calculations using $4\pi M_S = 14.3$ kG, $K_1 = -4.5 \times 10^5$ erg/cm³, $K_u = 9.0 \times 10^5$ erg/cm³, $K_p = -22 \times 10^5$ erg/cm³, $g = 2.1$, and $A = 1.4 \times 10^{-6}$ erg/cm. The modes are labeled B_2 , C , and D for reference. Calculated mode profiles (m_x) are also shown as functions of position in the film (of thickness h). The dotted line is the zero amplitude reference. The profiles are shown for $H_0 = 0.0, 2.4$, and 5.0 kOe.

K_p is also included in our description, but assumed to be small such that the equilibrium magnetization is in the film plane due to the demagnetizing energy of the film geometry (i.e., $K_p < -2\pi M_S^2$). The full equations of motion are given in Ref. 8.

Using the SQUID determined value for $4\pi M_S$, the exchange constant A , gyromagnetic ratio γ , and anisotropies K_1 , K_u , K_p were adjusted to provide a best fit to all the light scattering data. Each parameter controls a different aspect of the spin-wave frequencies. For example, the quantity $2A/M_S$ controls the relative frequencies of the different bulk modes, and small negative values of K_p lower the frequencies of all modes. The best fit parameter set was determined to be 1.4×10^{-6} erg/cm for A , 2.9 GHz/kOe for γ , -4.5×10^5 erg/cm³ for K_1 , 9.0×10^5 erg/cm³ for K_u , and -2.2×10^6 erg/cm³ for K_p . Calculations using the above parameter set are depicted in the same figures by dotted lines. The error on the measured frequencies is about ± 2 GHz.

Spin-wave frequencies as a function of H_0 applied along easy and hard directions are shown in Fig. 2. The low field behavior for H_0 applied in the hard direction is due to the

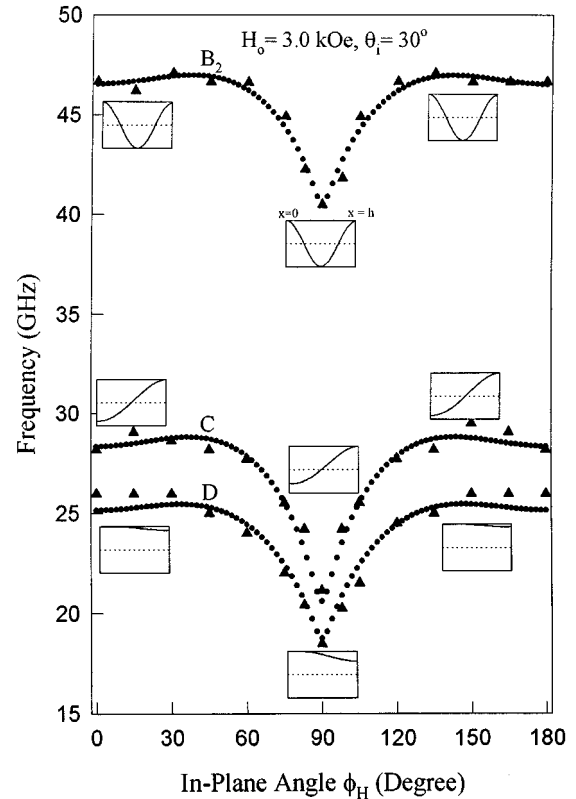


FIG. 3. In-plane angular dependence ϕ_H of the surface and two lowest bulk spin-wave frequencies. The applied magnetic field is 3.0 kOe and the angle of incidence θ_i was 30° . The dotted lines are calculations using the same parameters as in Fig. 2. The calculated mode profiles (m_x) are shown for $\phi_H = 0^\circ, 45^\circ$, and 90° .

magnetization not being aligned along the field direction. The magnetization is entirely along the hard direction only for field strengths greater than 2.4 kOe. This critical field coincides with a slight dip in the spin-wave frequencies. The value of 2.4 kOe is consistent with the hard direction saturation field found from hysteresis loop measurements. We also note that one can show using Eq. (1) that the saturation field in the hard direction is given by $2(K_u - K_1)/M_S$. Using the parameters given above, this equals 2.37 kOe, which is in good agreement with the magnetization and light scattering measurements.

Profiles are also shown in Fig. 2 for three modes labeled B_2 , C , and D at different fields. The profiles show how the amplitudes of the x components of the fluctuating magnetization, m_x , vary as a function of position in the film. The mode B_2 has a much weaker scattering intensity and is identified as a higher order $n=2$ bulk mode. For the parameters listed above, examination of the profiles shows that the lowest frequency mode D is surfacelike and mode C is the $n=1$ bulk mode. The inset in Fig. 2 shows the spin-wave frequencies as a function of H_0 , applied along the easy axis. The three modes increase approximately linearly with field and the slope is controlled by γ .

The data and calculations in Fig. 3 are for a constant applied field of 3.0 kOe that is sufficient to saturate the sample with H_0 in the hard direction (at $\phi_H = 90^\circ$). Mode profiles are again shown for the x component of the magnetization. The hybridization between the C and D modes is

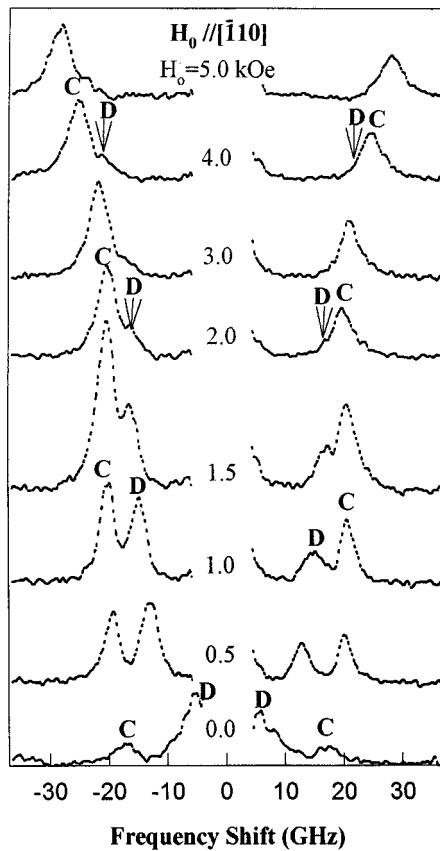


FIG. 4. Brillouin spectra of the 357 Å thick bcc Co film for different magnetic fields applied along the hard axis ($[110]$ direction). Note the shift of the maximum intensity from peak D to peak C as the field increases.

largest for ϕ_H near 90° . The behavior of the spin-wave frequencies with ϕ_H provides the primary evidence for a four-fold anisotropy. The maximum in the frequencies at 0 and 180° with a single minimum at 90° show a dominant second order uniaxial anisotropy, K_u . The sharpness of the minimum implies contributions from a higher order anisotropy.

Reproduction of the data around the minimum requires a negative K_1 . A negative K_1 places the fourfold easy axes along $[\bar{1}11]$ directions and the fourfold hard axes along the principle directions. For this orientation of the surface, a $[\bar{1}11]$ direction at 55° from the $[100]$ direction. This means that M_S prefers to stay near the $[\bar{1}11]$ direction even for ϕ_H fairly far from 55° . M_S therefore aligns along the field in the hard direction only for ϕ_H near 90° . The result is a narrow dip between 75° and 105° in Fig. 3, where M_S swings into the hard direction. The constant K_1 is still an order of magnitude smaller than K_u so additional structure due to the fourfold symmetry of K_1 is not visible on this scale. The observable hard and easy directions for the magnetization are therefore determined by the uniaxial anisotropy K_u .

The fits to the data presented in Figs. 2 and 3 are reasonable within the error of the measurements. Difficulties appear however when we attempt to understand the scattering intensities. The intensities for the field along the hard direction are shown in Fig. 4 for different values of H_0 . At low fields and high fields the identification of individual peaks becomes

ambiguous, but between 0.5 and 3 kOe, peak C clearly increases in intensity. This can be understood by considering how the surface mode depends on propagation direction. At low fields the magnetization is not aligned along the field and at zero field is perpendicular to the field direction. The scattering geometry however always measures spin waves with the propagation perpendicular to the field. Thus near zero field, the spin waves propagate parallel to the magnetization.

The most prominent feature in Brillouin spectra from ferromagnets is the Damon-Eshbach surface mode which only exists for a limited range of propagation directions around perpendicular to the magnetization. A surface localized mode is therefore not expected for small fields applied in the hard direction, and will only be observed in our scattering geometry for large fields when the magnetization aligns along the field. In this case the largest peak observed at small fields (less than 1.5 kOe) is thus the $n=0$ bulk mode.

These features are not entirely consistent with the intensities measured for different fields. We can see this by examining the negative frequency shifted anti-Stokes peaks in terms of the calculated profiles shown in Fig. 2. The profiles suggest that the lowest frequency mode D should have the largest intensity for all fields. This is because the amplitude of mode D varies the least across the film thickness. The measured anti-Stokes spectra in Fig. 4 instead show the middle frequency peak (C) to have the largest intensity for fields greater than 0.5 kOe. Note that the Stokes/anti-Stokes ratio for mode C increases with increasing field. This is because mode C becomes localized to the surface and means that the Stokes intensity for peak C is less than the Stokes intensity for peak D .

Additional difficulties appeared when we examined the intensities as a function of the angle ϕ_H at fixed field.¹⁶ The measured intensities indicated that the lowest frequency mode had the largest intensity for $\phi_H < 45^\circ$ and for $45^\circ < \phi_H < 90^\circ$, the middle frequency peak was observed to have the largest intensity. This behavior is not consistent with the mode profiles in Fig. 3 which show that the lowest frequency peak should have the largest scattering intensity for all angles.

This behavior would be consistent with a surface mode that was much less sensitive to ϕ_H than the bulk modes. If so, then near $\phi_H = 90^\circ$ the $n=1$ bulk mode could have a frequency lower than the surface mode, a frequency degenerate with the surface mode near 80° and 110° , and a frequency higher than the surface mode for all other angles. One way to have this kind of behavior would be for the internal fields near the surfaces to be different from those in the middle of the film. This would give rise to torques acting on spins near the surfaces that would shift the frequencies of the bulk modes by "pinning" the spins near the surfaces. The energy shift is primarily through the exchange contribution, and so the bulk modes are more strongly affected by pinning than the surface mode.¹⁷

Bulk mode pinning would also affect interpretation of the frequency versus field experiments. For small fields the magnetization is aligned mostly in the easy direction parallel to the wave vector. For these low fields, the largest intensity mode should be the uniform mode and have the lowest frequency. As the field increases and the magnetization moves

into the hard direction, pinning could lower the frequency of the $n=1$ bulk mode below that of the surface mode, thus leading to the middle frequency mode having the largest intensity.

We tested this idea by including a small surface anisotropy K_{sp} in the frequency calculation. We are able in fact to fit the data shown in Figs. 2 and 3 equally well, within experimental error, using either $K_{sp} = -0.15 \text{ erg/cm}^2$ or $K_{sp} = 0$ and $K_u = -2.2 \times 10^6 \text{ erg/cm}^3$. Unfortunately, calculated intensities (using the method of Cochran and Dutcher¹⁴) with simple surface pinning terms did not reproduce both the Stokes and anti-Stokes intensities.

We found qualitative agreement between the calculations and the data in Fig. 4 for the anti-Stokes processes only. The calculated Stokes peak intensities did not agree with the measured C and D peak intensities for fields below 1.5 kOe.¹⁶

A possible explanation for this discrepancy in the measured and calculated intensities may be linked with the unusually large linewidths sometimes observed in the spectra. Previous work suggests that Brillouin light scattering linewidths can narrow for certain orientations of the magnetization if there is a distribution of anisotropies.¹⁸ The well defined peaks in Fig. 4, which occur for cases where the magnetization is oriented between 0° and 90° from the $[100]$ axis may be due to reduced linewidths arising from a distribution of anisotropies.

Such a distribution would also mean that the Stokes/anti-Stokes ratios represent averages over spin waves traveling in

regions with different effective internal fields. In some regions the surface mode could have a higher frequency than the $n=1$ bulk mode, and the reverse in other regions. This would tend to blur the distinction between the low frequency C and D peaks in terms of their relative Stokes/anti-Stokes intensity ratios. Thus an alternative or additional explanation for the behavior of the observed intensities may involve a distribution of effective anisotropy fields that vary either in magnitude or direction.

A theoretical description for spin waves with a distribution of anisotropies would introduce additional parameters into the model. Although this would allow us to reproduce the measured intensities and frequencies, the amount of available data does not justify the inclusion of additional parameters in order to obtain a better fit. We note however that some evidence for inhomogeneous magnetic properties already exists. Neutron scattering experiments on bcc Co films grown directly on GaAs substrates suggest spatial variations in the magnetic moment.¹⁹ These variations in the magnetic moment could appear as changes in the effective internal fields.

In summary, we have examined the magnetic properties of a 357 Å thick bcc Co film using Brillouin light scattering. A large in-plane uniaxial anisotropy with the easy axis along the $[001]$ direction and a fourfold anisotropy were found. Unusual light scattering intensities were observed that may indicate a distribution of anisotropies and surface pinning fields in the Co film.

-
- ¹G. A. Prinz, Phys. Rev. Lett. **54**, 1051 (1985).
²G. R. Harp, R. F. C. Farrow, D. Weller, T. A. Rabedeau, and R. F. Marks, Phys. Rev. B **48**, 17 538 (1993).
³Y. U. Idzerda, D. M. Lind, D. A. Papaconstantopoulos, G. A. Prinz, B. T. Jonker, and J. J. Krebs, Phys. Rev. B **48**, 17 538 (1993).
⁴A. Y. Liu and D. J. Singh, Phys. Rev. B **47**, 8515 (1993).
⁵D. J. Singh, Phys. Rev. B **45**, 2258 (1992).
⁶Y. U. Idzerda, D. M. Lind, D. A. Papaconstantopoulos, G. A. Prinz, B. T. Jonker, and J. J. Krebs, Phys. Rev. Lett. **61**, 1222 (1988).
⁷R. E. Camley and M. Grimsditch, Phys. Rev. B **22**, 5420 (1980).
⁸S. Subramanian, X. Liu, R. L. Stamps, R. Sooryakumar, and G. A. Prinz, Phys. Rev. B **52**, 10 194 (1995).
⁹E. Gu, M. Gester, R. J. Hicken, C. Daboo, M. Tselepi, S. J. Gray, J. A. C. Bland, L. M. Brown, T. Thomson, and P. C. Riedi, Phys. Rev. B **52**, 14 704 (1995).
¹⁰X. Liu, R. L. Stamps, R. Sooryakumar, and G. A. Prinz, J. Appl. Phys. **79**, 5387 (1996).
¹¹S. Subramanian, R. Sooryakumar, G. A. Prinz, B. T. Jonker, and Y. U. Idzerda, Phys. Rev. B **49**, 17 319 (1994).
¹²R. E. Camley and D. L. Mills, Phys. Rev. B **18**, 4821 (1978).
¹³R. L. Stamps and B. Hillebrands, Phys. Rev. B **43**, 3532 (1991).
¹⁴J. R. Dutcher and J. F. Cochran, J. Magn. Magn. Mater. **72**, 307 (1988).
¹⁵G. Rupp, W. Wetzling, R. S. Smith, and W. Jantz, J. Magn. Magn. Mater. **45**, 404 (1984).
¹⁶X. Liu, Ph.D. thesis, The Ohio State University, 1996.
¹⁷G. T. Rado and J. R. Weertman, J. Phys. Chem. Solids **11**, 315 (1959).
¹⁸J. V. Harzer, B. Hillebrands, R. L. Stamps, G. Güntherodt, D. Weller, Ch. Lee, R. F. C. Farrow, and E. E. Marinero, J. Magn. Magn. Mater. **104-107**, 1863 (1992).
¹⁹J. A. C. Bland, R. C. Bateson, P. C. Riedi, R. G. Grahm, H. J. Lauter, J. Penfold, and C. Shackleton, J. Appl. Phys. **69**, 4989 (1991).